

## Activating Killer-cell Immunoglobulin-like Receptors are associated with the severity of COVID-19

Enrique Bernal<sup>1</sup>, Lourdes Gimeno<sup>2,3\*</sup>, María J. Alcaraz<sup>1\*</sup>, Ahmed A Quadeer<sup>4</sup>, Marta Moreno<sup>5</sup>, María V. Martínez-Sánchez<sup>2</sup>, José A. Campillo<sup>2</sup>, Jose M. Gomez<sup>5</sup>, Ana Pelaez<sup>6</sup>, Elisa García<sup>7</sup>, Maite Herranz<sup>5</sup>, Marta Hernández-Olivo<sup>8</sup>, Elisa Martínez-Alfaro<sup>9</sup>, Antonia Alcaraz<sup>1</sup>, Ángeles Muñoz<sup>1</sup>, Alfredo Cano<sup>1</sup>, Matthew R McKay<sup>4,10</sup>, Manuel Muro<sup>2</sup>, and Alfredo Minguela<sup>2,5</sup> and on behalf of Murcian COVID19 Study group.

From: <sup>1</sup>Infectious Disease Unit, Reina Sofia University Hospital and the Instituto Murciano de Investigación Biosanitaria (IMIB), Murcia, Spain; <sup>2</sup>Immunology Service, Hospital Clínico Universitario Virgen de la Arrixaca (HCUVA) and Instituto Murciano de Investigación Biosanitaria (IMIB), Murcia, Spain; <sup>3</sup>Human Anatomy Department, University of Murcia (UM), Murcia; <sup>4</sup>Department of Electronic and Computer Engineering, The Hong Kong University of Science and Technology, Hong Kong, China; <sup>5</sup>Internal Medicine Service, Hospital Universitario Morales Meseguer, Murcia, Spain; <sup>6</sup>Internal Medicine Service. Hospital Rafael Méndez. Lorca, Spain; <sup>7</sup>Infectious disease unit, Hospital Clínico Universitario Virgen de la Arrixaca (HCUVA) and Instituto Murciano de Investigación Biosanitaria (IMIB), Murcia, Spain; <sup>8</sup>Pneumology Service. Hospital Universitario Santa Lucía, Murcia, Spain; <sup>9</sup>Internal Medicine Service. Hospital General de Albacete. Albacete, Spain; <sup>10</sup>Department of Chemical and Biological Engineering, The Hong Kong University of Science and Technology, Hong Kong, China.

## FOOT NOTES

\*Lourdes Gimeno and Maria J. Alcaraz contributed equally to this article. <sup>‡</sup>Lead contact

**Corresponding Author:** Dr. Alfredo Minguela. Hospital Clínico Universitario Virgen de la Arrixaca, El Palmar, 30120-Murcia, Spain. Email: [alfredo.minguela@carm.es](mailto:alfredo.minguela@carm.es).

**Funding:** This work was funded by MINECO - Instituto de Salud Carlos III (COV20/00377); Co-funded by European Regional Development Fund (ERDF), “A way to make Europe”; M.J. Alcaraz was funded by Murcian Association for the Investigation and Study of Infection Diseases (AMIEI). M.V. Martínez-Sánchez was funded by the Asociación Pablo Ugarte (APU).

**Potential conflicts of interest.** All No reported conflicts of interest. All authors have submitted the ICMJE Form for Disclosure of Potential Conflicts of Interest. Conflicts that the editors consider relevant to the content of the manuscript have been disclosed.

## ABSTRACT

**Background:** Etiopathogenesis of the clinical variability of the coronavirus disease 2019 (COVID-19) remains mostly unknown. Here we investigate the role of Killer-cell Immunoglobulin-like receptor (KIR)/Human Leukocyte Antigen Class-I (HLA-I) interactions in the susceptibility and severity of COVID-19.

**Methods:** KIR and HLA-I genotyping and NK cell (NKc) receptors immunophenotyping in 201 symptomatic patients and 210 non-infected controls.

**Results:** NKCs with a distinctive immunophenotype, suggestive of recent activation (KIR2DS4<sup>low</sup> CD16<sup>low</sup> CD226<sup>low</sup> CD56<sup>high</sup> TIGIT<sup>high</sup> NKG2A<sup>high</sup>), expanded in patients with severe COVID-19. This was associated with a higher frequency of the functional A-telomeric activating KIR2DS4 in severe than mild/moderate patients and controls (83.7%, 55.7% and 36.2%,  $p < 7.7 \times 10^{-9}$ ). In mild/moderate patients HLA-B\*15:01 was associated with higher frequencies of activating B-telomeric KIR3DS1 compared to patients with other HLA-B\*15 subtypes and non-infected controls (90.9%, 42.9% and 47.3%,  $p < 0.002$ ,  $P_c = 0.022$ ). This strongly suggests that HLA-B\*15:01 specifically presenting SARS-CoV-2 peptides could form a neo-ligand interacting with KIR3DS1. Similarly, a putative neo-ligand for KIR2DS4 could arise from other HLA-I molecules presenting SARS-CoV-2 peptides expressed on infected/activated lung antigen presenting cells.

**Conclusions:** Our results support a crucial role of NKCs in the clinical variability of COVID-19 with specific KIR/Ligand interactions associated to disease severity.

**Keywords:** SARS-Cov-2, COVID-19 severity, NK cells, activating KIR receptors, HLA class-I

## INTRODUCTION

The new severe acute respiratory syndrome coronavirus-2 (SARS-CoV-2) associated with the coronavirus disease-2019 (COVID-19) emerged in Wuhan (China) and spread worldwide, creating a global pandemic and a historic health and economic crisis [1]. Clinical spectrum of COVID-19 ranges from asymptomatic to pneumonia and the appearance of multiple complications such as acute respiratory distress syndrome, multiple-organ failure and death [2].

Emerging studies on COVID-19 report low numbers of peripheral blood Natural Killer cells (NKCs) [3–5], but increased numbers infiltrating the lung [6]. NKCs are the first line of defense against viral infections. Moderate NKc activation promotes infection control, while stronger activation can be related to immunopathology [7]. NKc activation and function is regulated by the interplay between activating and inhibitory receptors [8]. In humans, natural cytotoxicity receptors (NKp30, NKp44 and NKp46) and DNAX Accessory Molecule-1 (DNAM-1/CD226) are activating receptors that recognize viral-derived/induced products [9]. NKCs can also recognize stress-induced ligands through the natural killer group 2 (NKG2) family, most notably NKG2D, which interacts with the MHC-class-I chain-related protein A/B (MICA/B) and UL16 binding-protein (ULBP). Human NKCs can also express up to 6 different activating Killer-cell Immunoglobulin-like Receptors (aKIR), KIR2DS1-5 and KIR3DS1, that recognize peptide-loaded Human Leukocyte Antigen class-I (HLA-I). Interactions of aKIRs have been reported between KIR2DS1/HLA-C2-allotypes [10], KIR2DS2/HLA-C1-allotypes [11], KIR2DS2/HLA-A\*11 [12], KIR2DS4/HLA-A\*11/C\*02/C\*04/C\*05/C\*16 [13] and KIR3DS1\*014/HLA-I alleles with Bw4 epitope [14]. HLA-F, which is upregulated in local macrophages during viral infections, is a ligand for KIR3DS1 and KIR2DS4 [15,16].

To regulate activating signals, a repertoire of inhibitory receptors that survey HLA-I repress NKCs to protect healthy cells from inappropriate killing [17]. Although it may seem contradictory, NKCs become fully competent during a process known as “licensing”, where inhibitory receptors interact with

their cognate HLA-ligands. Licensing inhibitory interactions include KIR2DL1/HLA-C2-allotypes, KIR2DL2-3/HLA-C1-allotypes, KIR3DL1/HLA-Bw4-allotypes, KIR3DL2/HLA-A\*03/A\*11 and NKG2A/HLA-E (revised in [18]).

KIR3DS1/Bw4 interaction, in absence of functional full-length exon-5 KIR2DS4 (fKIR2DS4), protects from HIV infection [19] and slows down progression to AIDS [20]. Telomeric activating KIR2DS1 and KIR3DS1 protect against cytomegalovirus infection after kidney transplantation [21]. In contrast, fKIR2DS4 is associated with increased risk of chronic HBV and HCV [22,23], as well as with high HIV loads and low CD4<sup>+</sup> T-cell counts [24], by promoting a pro-inflammatory state, since polyfunctional NKcs coexpressing CD107a, IFN- $\gamma$  and MIP-1 $\beta$  are highly enriched in fKIR2DS4 homozygous individuals [25].

Although KIR receptors and their HLA-ligands are among the most diverse molecules in nature and the repertoire of KIR/HLA-ligand interactions determines the susceptibility to infections, autoimmunity or cancer (<http://www.allelefreqencies.net/tools/kirDiseaseBib.aspx>), their role in COVID-19 clinical variable remains unexplored. This study shows how fKIR2SD4 is associated with severe COVID-19, while KIR3DS1 in presence of HLA-B\*15:01 is associated with mild/moderate COVID-19. These data support a decisive role of NKcs in the immunopathogenesis of COVID-19.

## **METHODS**

### **Study design and patients**

This cross-sectional prospective study enrolled 201 symptomatic COVID-19 patients and 210 sex-, age- and ethnicity-matched healthy controls. The Ethics Committee of General University Hospital Reina-Sofia (Spain) approved the study. Written consent was obtained from patients and controls. SARS-CoV-2 infection was confirmed by RT-PCR. Patients were included in the study once they reached clinical stability at day 75 (IQR61-92) and followed for 120 days from symptoms onset. SOFA

(Sequential Organ Failure Assessment) scale was used to assess disease severity [26]. The disease was considered severe when patients required invasive mechanical ventilation (IMV). Serum and EDTA blood samples were obtained to determine biochemical, microbiological, hematological and immunological variables.

### **HLA-A, -B and -C and KIR genotyping**

HLA-I and KIR genotyping was performed on DNA samples extracted with QIAamp-DNA-Blood-Mini-kit (QIAGEN-GmbH, Germany) using Lifecodes HLA-SSO and KIR-SSO kits (Immucor, Stamford, CT) and Luminex®. HLA-A, B and C genotyping allowed for identification of Bw4, C1, and C2 KIR-ligands [27]. Full-exon-5 (fKIR2DS4) and deleted-exon-5 (dKIR2DS4) KIR2DS4 alleles were identified. Centromeric and telomeric AA/Bx genotypes were identified [28].

### **Flow cytometry**

The expression of activating and inhibitory receptors on CD3-CD16<sup>-/+</sup>CD56<sup>++</sup> (CD56<sup>bright</sup>) and CD3-CD16<sup>+</sup>CD56<sup>+</sup> (CD56<sup>dim</sup>) NKc subsets and CD3<sup>+</sup>CD4<sup>+</sup> and CD3<sup>+</sup>CD4<sup>-</sup> T cells was evaluated as percentage of positive cells and as mean fluorescence intensity (MFI) using FACSLyric and DIVA-9.0 (Becton-Dickinson, BD) as described in figure 1.

### **Modeling B-telomeric aKIR affinity for HLA-B\*15 allotypes presenting SARS-CoV-2 peptides**

Modeling receptor/ligand affinity of B-telomeric aKIRs (KIR2DS1 and KIR3DS1) for HLA-B\*15 allotypes (B\*15:01, B\*15:03, B\*15:04, B\*15:17, B\*15:18, and B\*15:24) presenting SARS-CoV-2 peptides was done by casting it as a sequence alignment problem [29]. Affinity alignment scores were computed

using the PAM250 scoring matrix, with a high score indicating higher likelihood of binding. NetMHCpan-4.1 [30] was used with the Wuhan-Hu-2019 complete proteome reference sequence (GISAID ID: EPI\_ISL\_402125) to predict strong-binding 9-mer peptides presented for each HLA-B\*15 allotypes (percentile rank < 0.05 or score > 0.8, Supplementary File-1).

Since KIR3DS1 residues interacting with HLA-B\*15 presenting peptides have not been described, potential interacting residues (C-alpha  $\leq$  8Å) were obtained by using the structure of its homologous KIR3DL1 (with 97% amino acid similarity of extracellular domains [31]) in complex with HLA-B\*57:01 presenting peptide (PDB-ID: 5T70), and aligning the protein sequence of KIR3DL1 with that of KIR3DS1 (NCBI accession number: NP\_001077008.1). Interaction score between the receptor interacting residues and the SARS-CoV-2 peptide was obtained as the mean affinity alignment score of total interacting residues. Interaction score of KIR3DL1/KIR3DS1 with its Bw4 ligand [32] was calculated to ascertain the affinity of natural occurring KIR/ligand interactions. For this analysis, potential KIR3DS1 residues interacting with the Bw4 epitope (HLA-B positions 77, 80, 81, 82, and 83 [33]) were identified based on the structure of KIR3DL1 in complex with HLA-B\*57:01 (PDB ID: 3VH8).

Similar procedure was used to model KIR2DS1/HLA-B\*15-peptide interactions. KIR2DS1 interacting residues were obtained using KIR2DL1 structure in complex with HLA-Cw4 presenting a peptide (PDB-ID: 1IM9) [34] and aligning the protein sequence of KIR2DL1 with that of KIR2DS1 (NCBI accession number: XP\_011546300.1).

### **Statistical analysis**

Data were analyzed using SPSS-24.0 (SPSS-Inc., Chicago, IL). Categorical variables were analyzed using frequency tables and Pearson's- $\chi^2$  or two-tailed Fisher's exact tests. Bonferroni correction ( $P_c$ ) was applied when needed. Mean and standard deviation (SD) were used for continuous variables and differences were estimated with ANOVA, Student's-t or Mann-Whitney-U tests based on the presence or absence of normal distribution. Association between variables was assessed with

binary logistic regression analysis, adjusted for confounding variables. Variables with  $p < 0.05$  in the univariate regression analysis were included in the multivariate analysis. The impact of fKIR2DS4 on the mean time for admission to the intensive care unit (ICU) was assessed using Kaplan-Meier and the Mantel-Haenszel log-rank test. The time was censored 30 days after the onset of symptoms.  $P < 0.05$  was considered significant.

## RESULTS

### Patient characteristics according to IMV requirement

Table 1 summarizes biological, clinical and evolutionary characteristics of patients according to IMV requirements. Although no significant differences in age or sex were observed between patients requiring or not IMV, the former showed worst comorbidity and severity scores, biochemical and hematological parameters, more intense treatments and worst clinical evolution. Higher frequency of Caucasians than Latin-Americans required IMV probably due to their older age (59.0% vs. 53.5%,  $p = 0.019$ ).

### fKIR2DS4 is associated with severe COVID-19

First we explored the role of HLA-I allotypes in the susceptibility and severity of SARS-CoV-2 infection. Comparing controls and patients, we observed a protective role for HLA-A\*26 (10.8% vs. 5.5%) and HLA-A\*33 (7.4% vs. 2.0%), and a risk role for HLA-A\*23 (4.4% vs. 11.4%), HLA-A\*24 (14.3% vs. 22.9%) and HLA-C\*01 (3.4% vs. 6.5%). Significant differences disappeared after correction (Supplementary Table E1).

No differences were found either for inhibitory or activating KIRs, AA and Bx centromeric and telomeric genotypes, or HLA-ligands (C1, C2, Bw4, or KIR2DS4-ligands), except for fKIR2DS4, which showed higher frequency in COVID-19 patients than in controls (61.7% vs. 36.2%,  $P < 9.5 \times 10^{-6}$ ). Consequently fKIR2DS4 could be considered as a risk factor for symptomatic COVID-19. Besides, fKIR2DS4 was associated to severe diseases with frequencies of 83.7% vs. 56.3% for patients who did or did not require IMV ( $p < 0.001$ ) (Table 2).

Table 3 summarizes clinical characteristics and evolution of patients depending on the presence of fKIR2DS4. Although no differences in age, sex or ethnicity were observed according to the presence of fKIR2DS4, those patients with fKIR2DS4 presented with higher SOFA score ( $2.88 \pm 3.4$  vs.  $1.67 \pm 2.17$ ,  $p < 0.006$ ), higher frequency of  $\text{SOFA} \geq 6$  (24.2% vs. 7.9%,  $p < 0.007$ ), shorter time to hospital admission ( $7.36 \pm 5.79$  vs.  $9.4 \pm 4.66$  days,  $p < 0.019$ ), higher frequency of admission (48.4% vs. 32.5%,  $p < 0.038$ ), higher frequency of kidney failure (17.7% vs. 5.6%,  $p < 0.03$ ) and longer ICU hospitalization ( $23.7 \pm 21.15$  vs.  $16.6 \pm 14.04$  days,  $p < 0.031$ ). No differences were detected in the treatment administered to moderate or severe Covid19 patients according to the presence of fKIR2DS4.

fKIR2DS4 was an independent variable able to predict: 1) need for IMV (OR=4.74,  $p < 0.002$ ) together with cardiovascular disease (OR=4.23,  $p < 0.003$ ), ferritin (OR=1.0,  $p < 0.005$ ) and D-dimer (OR=1.0,  $p < 0.008$ ) (Figure 2A); and 2) ICU admission (OR=2.51,  $p < 0.031$ ) together with cardiovascular disease (OR=3.94,  $p < 0.014$ ) and D-dimer (OR=1.0,  $p < 0.005$ ). Shorter median time to ICU admission was observed for patients with fKIR2DS4 ( $20.5 \pm 11$  vs.  $24.1 \pm 10$  days,  $p < 0.027$ ) (Figure 2B).

### **KIR2DS4<sup>+</sup> NKCs with a distinctive immunophenotype were expanded in COVID-19**

To understand the relationship that KIR2DS4<sup>+</sup> NKCs may have with disease severity, leukocyte subtypes and KIR<sup>+</sup> NKc repertoire were analyzed in healthy controls and patients without or with IMV. To avoid the sequelae of intense treatments applied to patients with severe disease the cellular study was performed at day 75 (IQR61-92) after hospital discharge. However, compared to controls, patients

presented reduced numbers of lymphocytes (27.4%, 25.2%, and 20.2%,  $p < 0.01$ ), non-classical monocytes (16.7%, 15.7%, and 12.6%,  $p < 0.01$ ), neutrophils (40.3%, 38.1%, 33.7%,  $p < 0.05$ ), and CD4<sup>+</sup> T-lymphocytes (33.7%, 29.4%, and 25.6%,  $p < 0.001$ ), and increased numbers of CD8<sup>+</sup> T-lymphocytes (23.9%, 28.5%, 30.0%,  $p < 0.05$ ). These values were accentuated in patients with IMV (Figure 3A).

Although the numbers of CD56<sup>bright</sup> and CD56<sup>dim</sup> NKCs as well as the repertoire of KIR<sup>+</sup> NKCs did not show significant differences between controls and patients, NKCs expressing KIR2DS4 as the only KIR receptor (single-KIR2DS4<sup>+</sup>) showed higher frequency in patients requiring IMV than in patients without IMV and controls (9.1%, 5.1%, and 4.3%,  $p < 0.05$ ) (Figure 3B). When the expression as MFI of each KIR was studied in single-KIR<sup>+</sup> NKCs, no differences were found between the three study groups for KIR2DL1<sup>+</sup>, KIR2DL2/S2<sup>+</sup>, KIR2DL3<sup>+</sup>, KIR2DS1<sup>+</sup>, or KIR3DS1<sup>+</sup> NKCs, whereas a slight increase of KIR3DL1 was found in patients requiring IMV compared to those that did not or to controls (7869.5, 6076.1 and 6083.9, MFI,  $p < 0.01$ ). However, the expression of KIR2DS4 showed a prominent down-modulation in both groups of patients compared to controls (5392.5, 6500 and 8721.6 MFI,  $p < 0.001$ ) (Figure 3C). Since the expression of KIR receptors is down-modulated when interacting with their specific HLA-I ligand [35], we analyzed the expression of KIRs in presence of their HLA-ligands in COVID-19 patients. As already described, the presence of C2-ligand very significantly induced the down-modulation of KIR2DL1 (1847.5 vs. 1296.8,  $p < 0.001$ ). However, C1-ligands, Bw4-ligands and HLA-A\*11/C\*2/C\*4/C\*5/C\*16 induced slight non-significant down-modulations of their respective KIR2DL2/S2-L3, KIR3DL1 and KIR2DS4 receptors (Figure 3D). Therefore, the strong down-modulation observed for KIR2DS4 in COVID-19 patients did not appear to be associated with the presence of its HLA-ligands.

Additional immunophenotypic characteristics of KIR2DS4<sup>+</sup> NKCs are shown in Figure 3E. CD16 expression showed no differences between patients and controls, but, in general, NKCs expressing aKIRs (KIR2DS1, KIR3DS1 or KIR2DS4) showed lower levels of CD16 than NKCs expressing iKIRs ( $p < 0.05$ ). CD56 expression was higher in patients than in controls on NKCs expressing activating

KIR2DS1 ( $p < 0.01$ ), KIR3DS1 ( $p < 0.001$ ) and KIR2DS4 ( $p < 0.05$ ), but not on NKcs expressing iKIRs. CD226 expression was higher on all NKc subsets in patients that did not require IVM ( $p < 0.01$ , for all KIR<sup>+</sup> subsets) than in controls and patients with IMV. CD226 showed lower expression on NKcs bearing aKIRs than in those bearing iKIRs ( $p < 0.001$ ). NKG2D expression was lower in patients than in controls for all NKc subsets, with reductions statistically significant on KIR2DL1<sup>+</sup> ( $p < 0.05$ ), KIR2DL3<sup>+</sup> ( $p < 0.01$ ) or KIR2DS1<sup>+</sup> ( $p < 0.001$ ) NKc subsets. In contrast, TIGIT expression was higher in patients (particularly in patients with IMV) than in controls ( $p < 0.05$ , for all KIR<sup>+</sup> subsets). Finally, although no significant differences were found between controls and patients in NKG2A expression, in general, KIR2DS4<sup>+</sup> NKcs showed higher NKG2A expression than KIR3DS1<sup>+</sup> ( $p < 0.01$ ) and the other KIR<sup>+</sup> NKc subsets ( $p < 0.001$ ). Altogether, KIR2DS4<sup>+</sup> NKcs in severe COVID-19 showed a distinctive phenotype different from other NKc subsets consisting in KIR<sup>low</sup> CD16<sup>low</sup> CD226<sup>low</sup> CD56<sup>high</sup> TIGIT<sup>high</sup> NKG2A<sup>high</sup>.

### **B-telomeric aKIRs are associated to milder COVID-19 in HLA-B\*15:01 patients**

Since the frequency of KIR2DS4-ligands HLA-A\*11, C\*02, C\*04, C\*05, and C\*16 [36], all together or individually, did not show differences between controls and patients, we studied other putative HLA-ligands. Frequency of fKIR2DS4 remained within the ranges described for the global COVID-19 group (61.7%) for all HLA-A, -B, or -C allotypes, except for HLA-B\*15, where the frequency of fKIR2DS4 was lower than that observed in HLA-B\*15 controls (16.7% vs. 40.9%,  $p < 0.093$ ). In contrast, the frequency of fKIR2DS4 in HLA-B\*15 negative patients and controls remained unaltered (66.5% vs. 35.7%,  $p < 3.1 \times 10^{-9}$ ). To understand why it could be happening, the frequency of each KIR-receptor was evaluated in HLA-B\*15 positive and negative controls and patients (Figure 4A). Higher frequency of B-telomeric KIR-receptors KIR2DL5 (77.8% vs. 45.5%,  $p < 0.039$ ,  $P_c = 0.429$ ), KIR2DS1 (72.2% vs. 27.3%,  $p < 0.006$ ,  $P_c = 0.066$ ), KIR2DS5 (66.7% vs. 23.8%,  $p < 0.006$ ,  $P_c = 0.066$ ), KIR3DS1 (72.2% vs. 22.7%,  $p < 0.002$ ,  $P_c = 0.022$ ), and the Bx-telomeric genotype (72.2% vs. 22.7%,  $p < 0.002$ ,  $P_c = 0.022$ ) was

observed in HLA-B\*15 patients than controls. However, the frequency of all KIR-receptors remained unaltered in HLA-B\*15 negative patients and controls. In contrast, the frequency of KIR3DL1 (A-telomeric) was reduced in HLA-B\*15 patients compared to controls (66.7% vs. 100%,  $p < 0.005$ ,  $P_c = 0.055$ ). In a higher resolution analysis, it was found that in COVID-19 patients telomeric-aKIRs were specifically associated with HLA-B\*15:01, but not with other HLA-B\*15 subtypes (HLA-B\*15:03, B\*15:04, B\*15:17, B\*15:18, B\*15:24). Thus, compared to HLA-B\*15:01 healthy controls the frequencies of KIR2DS1 (27.3% vs. 90.9%,  $p < 0.001$ ,  $P_c = 0.011$ ), KIR2DS5 (22.7% vs. 81.8%,  $p < 0.002$ ,  $P_c = 0.022$ ) and KIR3DS1 (22.7% vs. 90.9%,  $p < 0.0003$ ,  $P_c = 0.0033$ ) were much higher in HLA-B\*15:01 patients. No significant differences were found between patients and controls with other HLA-B\*15 subtypes.

To further ascertain putative B-telomeric aKIR/HLA-B\*15 interactions, we used a computational approach [29] to model the affinity (interaction scores) for each HLA-B\*15 subtype (Figure 4B). HLA-B\*15:01 presenting SARS-CoV-2 peptides had higher interaction scores, and thus was more likely to interact with KIR3DS1, than HLA-B\*15:03 ( $p < 0.05$ ), HLA-B\*15:04 (no peptides found for this allotype), HLA-B\*15:17 ( $p < 0.001$ ), HLA-B\*15:18 ( $p = 0.1$ ), and HLA-B\*15:24 ( $p < 0.05$ ). Interaction scores for KIR3DS1/HLA-B\*15:01 were found to be within the range for its usual Bw4-ligand [32]. Besides, interaction scores for KIR2DS1/HLA-B\*15:01 presenting SARS-CoV-2 peptides were much lower than those of KIR3DS1 ( $p < 0.0001$ ), pointing KIR3DS1 as the most likely receptor interacting with HLA-B\*15:01.

Bx-telomeric genotype was more frequent in HLA-B\*15:01 patients that did not require IMV (84.6% vs. 15.4%,  $p = 0.09$ ), and therefore it was associated with milder COVID-19, which is reasonable since the frequency of the A-telomeric fKIR2DS4 (associated to severe disease) was decreased in these patients.

## DISCUSSION

The biological cause of COVID-19 clinical variability remains mostly unknown. This study investigated in COVID-19 the role of receptors that regulate the function of NKCs, which together with their HLA-ligands, are some of the most variable molecules in nature (<http://www.allelefreqencies.net/>). Results show that telomeric-aKIRs, fKIR2SD4 by itself and KIR3DS1 in presence of HLA-B\*15:01, are associated with severe and mild/moderate COVID-19, respectively. These results also support a decisive role of NKCs in the pathogenesis and clinical variability of COVID-19.

Functionality and number of NKCs are significantly decreased in COVID-19 [3,4,37], and yet the underlying causes have not been explored. During the acute phase of the infection peripheral blood NKCs increase the express of inhibitory (NKG2A), regulatory (TIM-3) and exhaustion (PD-1) molecules and reduce the expression of activating receptors (DNAM-1 and NKG2D) and the secretion of IFN $\gamma$  [38]. Two months after infection, some of these effects were still observed in patients from our study, particularly in those requiring IMV: reduced number of total lymphocytes, non-classical monocytes, neutrophils and CD4<sup>+</sup> T-cell and increased number of CD8<sup>+</sup> T-cells and single-KIR2DS4<sup>+</sup> NKCs. These single-KIR2DS4<sup>+</sup> NKCs showed a distinctive phenotype with a clear down-modulation of its KIR compared to healthy controls, most probably due to active interaction with specific ligands. KIRs are generally down-modulated when interacting with their HLA-ligand [35]. Although in our study KIR/HLA-ligand-induced down-modulation was observed for most single-KIR<sup>+</sup> NKc subsets, down-modulation induced by normal-constitutive HLA-I expression was much lower than that observed in single-KIR2DS4<sup>+</sup> NKCs, suggesting that KIR2DS4 might interact with unconventional ligands. Like other single-aKIR<sup>+</sup> NKc subsets (KIR2DS1<sup>+</sup> and KIR3DS1<sup>+</sup>), single-KIR2DS4<sup>+</sup> NKCs showed reduced expression of CD16, CD226 and NKG2D, but highly expressed CD56 and TIGIT, suggesting that these cells had been recently involved in an activation event [39,40]. Supporting this idea is the NKG2A over-expression specifically observed in single-KIR2DS4<sup>+</sup> NKCs, which is consistent with the strong NKG2A

over-expression described during the acute phase [41] and supports a primary role of KIR2DS4<sup>+</sup> NKcs in the SARS-CoV-2 response.

In fact, the frequency of fKIR2DS4 gene was significantly increased in all COVID-19 patients, and particularly in those requiring IMV, 83.7% vs. 36.2% in controls. It has been recently suggested that frequency of HLA-C\*05 (a KIR2DS4 ligand) was related to mortality variability in different COVID-19 populations [42]. However, in our series no differences between patients and controls were observed in the frequency of HLA-C\*05 or KIR2DS4/HLA-C\*05 interaction. In fact, fKIR2DS4 frequency did not change in patients bearing its putative ligands (HLA-A\*11/C\*02/C\*04/C\*05/C\*16 [36]), which suggests that new ligands could be interacting with KIR2DS4 in COVID-19 patients. In 2013 Goodridge *et al.* suggested that open-conformer HLA-F could be a ligand for KIR2DS4 [43]; however, more recent results demonstrate that HLA-F open-conformer is a ligand for KIR3DS1 and KIR3DL2 but not for KIR2DS4 [44]. In contrast, peptide-bound HLA-F is not a ligand for KIR3DS1 because peptides directly hinder KIR3DS1/HLA-F interaction [44]. However, it is possible that a SARS-CoV-2 peptide presented in HLA-F could form a neo-ligand for KIR2DS4, in the same way that HLA-C\*05:01 does present bacterial 9-mer peptides carrying a tryptophan at position-8 to become a ligand for KIR2DS4 [45]. Indeed, HLA-F can present peptides of unconventional length dictated by the R62W mutation that produce an open-ended groove accommodating long peptides [44]. In contrast, this putative neo-ligand formed by HLA-F presenting SARS-CoV-2 peptides will not be recognized by KIR3DS1, as previously indicated [44] and supported by our data, since the frequency of KIR3DS1 in COVID-19 patients did not differ from that in controls.

HLA-F is mainly expressed in activated lymphocytes and monocytes [46]. Alveolar macrophages, the predominant leukocytes in the lung, are strongly activated in COVID-19 patients and include viral particles within their cytoplasm [47], and therefore, they would be able to present SARS-CoV-2 peptides in HLA-F. Besides, SARS-CoV-2 induces the expression of CXCR3 ligands (CXCL9-11) in lung tissue [48] and macrophages [5] facilitating NKc recruitment from the peripheral blood [37].

Once in the lung, NKcs could interact with neo-ligands expressed in activated macrophages, as suggested by the down-modulation of its KIR2DS4 receptor. The activation of this polyfunctional KIR2DS4<sup>+</sup> NK could promote a pro-inflammatory environment that would impair the resolution of the infection as it does in HIV, HCV and HBV infections [22–24].

In the search for new possible KIR2DS4 ligands, we tested all HLA-A, B, or C allotypes, and except for HLA-B\*15, none altered the frequency of fKIR2DS4 observed in total patients. HLA-B\*15 was associated with very low frequency of fKIR2DS4, lower than that in controls, which led us to investigate potential interactions of HLA-B\*15 with other KIRs. HLA-B\*15:01 allotype, but not other HLA-B\*15 allotypes (HLA-B\*15:03, \*15:04, \*15:17, \*15:18, \*15:24), was specifically associated with much higher frequencies of B-telomere aKIRs (KIR2DS1 and KIR3DS1). This strongly suggests the appearance of a second neo-ligand, in this case HLA-B\*15:01 presenting a SARS-CoV-2 peptide, that would be recognized by KIR3DS1. This hypothesis is supported by a computational approach to model the affinity of B-telomeric aKIR/HLA-B\*15 interactions. Although this model relies on the assumption that interacting residues for KIR3DS1 and KIR2DS1 are similar to those of their respective inhibitory counterparts, KIR3DL1 and KIR2DL1 [49], it identified KIR3DS1 as the most likely receptor interacting with HLA-B\*15:01 presenting SARS-CoV-2 peptides. Besides, higher frequency of the HLA-B\*15:01 allotype in Latin-American than Caucasoid patients (13.3% vs. 4.1%), apart from their younger age (52.9 vs. 58.7 years), might have been reasons a milder disease was observed in patients of this ethnic group.

In comparison with other respiratory viruses, SARS-CoV-2 drives an unusual antiviral transcriptional response with low expression of IFN-I and IFN-III and high of chemokine (CXCLs) and inflammatory cytokines (IL1 and IL6), which could explain the proinflammatory state associated with COVID-19 [50]. This also suggests that non-classical receptor/ligand interactions could be operating, as our data seem to indicate. Nonetheless, to overcome main limitations of this study, such as the limited number of patients or the absence of functional studies, it would be necessary to conduct further

research that consistently confirm the interaction of KIR2DS4/HLA-F and KIR3DS1/HLA-B\*15:01 presenting SARS-CoV-2 peptides. However, our results suggest that this atypical virosis that requires immunosuppression to treat patient, may be related to the presence of neo-ligands that induce unusual antiviral responses. These results support a crucial role of NKcs in COVID-19 clinical variability and could be pointing to molecular targets useful for the development of specific treatments in this ill-fated disease.

### **Acknowledgments**

To Teresa Escámez Martínez director of the Biobanc-IMIB for her help in storing samples. To the health professionals involved in the extraction and shipment of samples.

Accepted Manuscript

## References

1. Zhou P, Yang X-L, Wang X-G, et al. A pneumonia outbreak associated with a new coronavirus of probable bat origin. *Nature*. **2020**; 579(7798):270–273.
2. Guan W-J, Ni Z-Y, Hu Y, et al. Clinical Characteristics of Coronavirus Disease 2019 in China. *N Engl J Med*. **2020**; 382(18):1708–1720.
3. Wilk AJ, Rustagi A, Zhao NQ, et al. A single-cell atlas of the peripheral immune response in patients with severe COVID-19. *Nat Med*. **2020**; 26(7):1070–1076.
4. Jiang Y, Wei X, Guan J, et al. COVID-19 pneumonia: CD8+ T and NK cells are decreased in number but compensatory increased in cytotoxic potential. *Clin Immunol*. **2020**; 218:108516.
5. Liao M, Liu Y, Yuan J, et al. Single-cell landscape of bronchoalveolar immune cells in patients with COVID-19. *Nat Med*. **2020**; 26(6):842–844.
6. Chua RL, Lukassen S, Trump S, et al. COVID-19 severity correlates with airway epithelium-immune cell interactions identified by single-cell analysis. *Nat Biotechnol*. **2020**; 38(8):970–979.
7. Waggoner SN, Cornberg M, Selin LK, Welsh RM. Natural killer cells act as rheostats modulating antiviral T cells. *Nature*. **2011**; 481(7381):394–8.
8. Lanier LL. Up on the tightrope: natural killer cell activation and inhibition. *Nat Immunol*. **2008**; 9(5):495–502.
9. Brandstadter JD, Yang Y. Natural killer cell responses to viral infection. *J Innate Immun*. **2011**; 3(3):274–9.
10. Fauriat C, Ivarsson M a, Ljunggren H, Malmberg K, Michae J. Education of human natural killer cells by activating killer cell immunoglobulin-like receptors. *Blood*. **2010**; 115(6):1166–1174.

11. David G, Djaoud Z, Willem C, et al. Large Spectrum of HLA-C Recognition by Killer Ig-like Receptor (KIR)2DL2 and KIR2DL3 and Restricted C1 Specificity of KIR2DS2: Dominant Impact of KIR2DL2/KIR2DS2 on KIR2D NK Cell Repertoire Formation. *J Immunol.* **2013**; 191(9):4778–4788.
12. Liu J, Xiao Z, Ko HL, Shen M, Ren EC. Activating killer cell immunoglobulin-like receptor 2DS2 binds to HLA-A\*11. *Proc Natl Acad Sci U S A.* **2014**; 111(7):2662–7.
13. Graef T, Moesta AK, Norman PJ, et al. KIR2DS4 is a product of gene conversion with KIR3DL2 that introduced specificity for HLA-A\*11 while diminishing avidity for HLA-C. *J Exp Med.* **2009**; 206(11):2557–72.
14. Graldine M O'Connor, Eriko Yamada, Andy Rampersaud, Rasmi Thomas M, Carrington A, McVicar DW. Analysis of binding of KIR3DS1\*014 to HLA Suggests Distinct Evolutionary History of KIR3DS1. *J Immunol.* **2011**; 187(5):2162–2171.
15. Garcia-Beltran WF, Hölzemer A, Martrus G, et al. Open conformers of HLA-F are high-affinity ligands of the activating NK-cell receptor KIR3DS1. *Nat Immunol.* **2016**; 17(9):1067–74.
16. Lunemann S, Schöbel A, Kah J, et al. Interactions Between KIR3DS1 and HLA-F Activate Natural Killer Cells to Control HCV Replication in Cell Culture. *Gastroenterology.* **2018**; 155(5):1366-1371.e3.
17. Long EO. Negative signaling by inhibitory receptors: The NK cell paradigm. *Immunol Rev.* **2008**; 224(1):70–84.
18. Guillamón CF, Martínez-Sánchez MV, Gimeno L, et al. NK Cell Education in Tumor Immune Surveillance: DNAM-1/KIR Receptor Ratios as Predictive Biomarkers for Solid Tumor Outcome. *Cancer Immunol Res.* **2018**; 6(12):1537–1547.

19. Jackson E, Zhang CX, Kiani Z, et al. HIV exposed seronegative (HESN) compared to HIV infected individuals have higher frequencies of telomeric Killer Immunoglobulin-like Receptor (KIR) B motifs; Contribution of KIR B motif encoded genes to NK cell responsiveness. *PLoS One*. **2017**; 12(9):e0185160.
20. Ivarsson MA, Michaëlsson J, Fauriat C. Activating killer cell Ig-like receptors in health and disease. *Front Immunol*. **2014**; 5(APR):1–9.
21. Stern M, Hadaya K, Hönger G, et al. Telomeric rather than centromeric activating KIR genes protect from cytomegalovirus infection after kidney transplantation. *Am J Transplant*. **2011**; 11(6):1302–1307.
22. Auer ED, Tong H Van, Amorim LM, et al. Natural killer cell receptor variants and chronic hepatitis B virus infection in the Vietnamese population. *Int J Infect Dis*. **2020**; 96:541–547.
23. Podhorzer A, Dirchwolf M, Machicote A, et al. The Clinical Features of Patients with Chronic Hepatitis C Virus Infections Are Associated with Killer Cell Immunoglobulin-Like Receptor Genes and Their Expression on the Surface of Natural Killer Cells. *Front Immunol*. **2017**; 8:1912.
24. Olvera A, Pérez-Álvarez S, Ibarrodo J, et al. The HLA-C\*04:01/KIR2DS4 gene combination and human leukocyte antigen alleles with high population frequency drive rate of HIV disease progression. *Aids*. **2015**; 29(5):507–517.
25. Merino AM, Dugast A-S, Wilson CM, et al. KIR2DS4 promotes HIV-1 pathogenesis: new evidence from analyses of immunogenetic data and natural killer cell function. *PLoS One*. **2014**; 9(6):e99353.
26. Singer M, Deutschman CS, Seymour CW, et al. The Third International Consensus Definitions for Sepsis and Septic Shock (Sepsis-3). *JAMA*. **2016**; 315(8):801–10.

27. Mandelboim O, Reyburn HT, Valés-Gómez M, et al. Protection from lysis by natural killer cells of group 1 and 2 specificity is mediated by residue 80 in human histocompatibility leukocyte antigen C alleles and also occurs with empty major histocompatibility complex molecules. *J Exp Med.* **1996**; 184(3):913–22.
28. Hsu KC, Chida S, Geraghty DE, Dupont B. The killer cell immunoglobulin-like receptor (KIR) genomic region: gene-order, haplotypes and allelic polymorphism. *Immunol Rev.* **2002**; 190:40–52.
29. Ogishi M, Yotsuyanagi H. Quantitative Prediction of the Landscape of T Cell Epitope Immunogenicity in Sequence Space. *Front Immunol.* **2019**; 10:827.
30. Reynisson B, Alvarez B, Paul S, Peters B, Nielsen M. NetMHCpan-4.1 and NetMHCIIpan-4.0: improved predictions of MHC antigen presentation by concurrent motif deconvolution and integration of MS MHC eluted ligand data. *Nucleic Acids Res.* **2020**; 48(W1):W449–W454.
31. O'Connor GM, Vivian JP, Gostick E, et al. Peptide-Dependent Recognition of HLA-B\*57:01 by KIR3DS1. *J Virol.* **2015**; 89(10):5213–21.
32. Lutz CT. Human leukocyte antigen Bw4 and Bw6 epitopes recognized by antibodies and natural killer cells. *Curr Opin Organ Transplant.* **2014**; 19(4):436–41.
33. Grifoni A, Montesano C, Patronov A, Colizzi V, Amicosante M. Immunoinformatic docking approach for the analysis of KIR3DL1/HLA-B interaction. *Biomed Res Int.* **2013**; 2013:283805.
34. Fan QR, Long EO, Wiley DC. Crystal structure of the human natural killer cell inhibitory receptor KIR2DL1-HLA-Cw4 complex. *Nat Immunol.* **2001**; 2(5):452–60.
35. Guillamón CF, Martínez-Sánchez M V, Gimeno L, et al. NK Cell Education in Tumor Immune Surveillance: DNAM-1/KIR Receptor Ratios as Predictive Biomarkers for Solid Tumor Outcome.

- Cancer Immunol Res. **2018**; <http://can>.
36. Nowak J, Kościńska K, Mika-Witkowska R, et al. Role of Donor Activating KIR-HLA Ligand-Mediated NK Cell Education Status in Control of Malignancy in Hematopoietic Cell Transplant Recipients. *Biol Blood Marrow Transplant*. **2015**; 21(5):829–39.
  37. Vabret N, Britton GJ, Gruber C, et al. Immunology of COVID-19: Current State of the Science. *Immunity*. **2020**; 52(6):910–941.
  38. Varchetta S, Mele D, Oliviero B, et al. Unique immunological profile in patients with COVID-19. *Cell Mol Immunol*. **2020**; .
  39. Acker HH Van, Capsomidis A, Smits EL, Tendeloo VF Van. CD56 in the immune system: More than a marker for cytotoxicity? *Front Immunol*. **2017**; 8(JUL):1–9.
  40. Yin X, Liu T, Wang Z, et al. Expression of the Inhibitory Receptor TIGIT Is Up-Regulated Specifically on NK Cells With CD226 Activating Receptor From HIV-Infected Individuals. *Front Immunol*. **2018**; 9(10):2341.
  41. Zheng M, Gao Y, Wang G, et al. Functional exhaustion of antiviral lymphocytes in COVID-19 patients. *Cell Mol Immunol*. **2020**; 17(5):533–535.
  42. Sakuraba A, Haider H, Sato T. Population Difference in Allele Frequency of HLA-C\*05 and Its Correlation with COVID-19 Mortality. *Viruses*. **2020**; 12(11).
  43. Goodridge JP, Burian A, Lee N, Geraghty DE. HLA-F and MHC class I open conformers are ligands for NK cell Ig-like receptors. *J Immunol*. **2013**; 191(7):3553–62.
  44. Dulberger CL, McMurtrey CP, Hölzemer A, et al. Human Leukocyte Antigen F Presents Peptides and Regulates Immunity through Interactions with NK Cell Receptors. *Immunity*. **2017**; 46(6):1018-1029.e7.

45. Sim MJW, Rajagopalan S, Altmann DM, Boyton RJ, Sun PD, Long EO. Human NK cell receptor KIR2DS4 detects a conserved bacterial epitope presented by HLA-C. *Proc Natl Acad Sci U S A*. **2019**; 116(26):12964–12973.
46. Lee N, Ishitani A, Geraghty DE. HLA-F is a surface marker on activated lymphocytes. *Eur J Immunol*. **2010**; 40(8):2308–18.
47. Pandolfi L, Fossali T, Frangipane V, et al. Broncho-alveolar inflammation in COVID-19 patients: a correlation with clinical outcome. *BMC Pulm Med*. **2020**; 20(1):301.
48. Chu H, Chan JF-W, Wang Y, et al. Comparative Replication and Immune Activation Profiles of SARS-CoV-2 and SARS-CoV in Human Lungs: An Ex Vivo Study With Implications for the Pathogenesis of COVID-19. *Clin Infect Dis*. **2020**; 71(6):1400–1409.
49. Vivian JP, Duncan RC, Berry R, et al. Killer cell immunoglobulin-like receptor 3DL1-mediated recognition of human leukocyte antigen B. *Nature*. **2011**; 479(7373):401–5.
50. Blanco-Melo D, Nilsson-Payant BE, Liu W-C, et al. Imbalanced Host Response to SARS-CoV-2 Drives Development of COVID-19. *Cell*. **2020**; 181(5):1036-1045.e9.

## Figure Legends

### Figure 1. Analysis of activating and inhibitory receptors on peripheral blood NK and T cells.

Staining protocol included 12-color/15-monoclonal antibody: CD3-BV510 (SK7, BD), CD4-BV786 (RPA-T4, BD), CD16-AF700 (3G8, BD), CD56-BV711 (NCAM16.2, BD), KIR2DL1/S1-PECy7 (EB6, BD), KIR2DL2/L3/S2-PE-Cy5 (GL183, Beckman-Coulter), KIR2DL1-FITC (143211, R&D-systems), KIRDL3-APC (180701, R&D-systems, KIR2DL3), KIR3DL1-APC (DX9, R&D-systems), KIR2DS4-APC (FES172, Beckman-Coulter), CD226-PE (11A8, Biolegend), NKG2A-BV786 (131411, BD), NKG2D-APC-Cy7 (1D11, Biolegend), and TIGIT-BV421 (741182, BD). NK and T cell subsets were identified following a hierarchical and logical gating strategy in Diva 9.0 software (BD): singlet cells were selected in a FSC-H/FSC-A dot plot (not shown), then lymphocytes were selected based on low dispersion for FSC/SSC and all lymphocyte subsets were hierarchically dependent on these gates. CD3<sup>+</sup> lymphocytes were gated as CD3<sup>+</sup>CD56<sup>-/+</sup> cells. CD3<sup>+</sup>CD4<sup>+</sup> and CD3<sup>+</sup>CD4<sup>-</sup> T cell subsets were set within CD3<sup>+</sup> lymphocytes. Total NKs were defined combining a CD3<sup>+</sup>CD56<sup>+</sup> gate with a CD56<sup>+/+</sup>CD16<sup>-/+</sup> gate. To exclude M2-monocytes in the NKc subset CD16<sup>++</sup>CD56<sup>-</sup> events were gated-out. The expression of KIR receptors (KIR2DS1<sup>+</sup>, KIR2DL1<sup>+</sup>, KIR2DL1<sup>+</sup>S1<sup>+</sup>, KIR2DL2/S2<sup>+</sup>, KIR2DL3<sup>+</sup>, KIR3DL1<sup>+</sup>, KIR3DS1<sup>+</sup> and KIR2DS4<sup>+</sup>) were estimated on total NKc and on CD8<sup>+</sup> T Lymphocytes. KIR2DL3<sup>+</sup>, KIR3DL1<sup>+</sup>, and KIR2DS4<sup>+</sup> cells (all of them stained with APC MoAbs) were separated by combining not-KIR2DL2/L3/S2 (in PE-Cy5) and not-KIR3DL1/S1 (in PE) gates, respectively. A special analysis was applied to patients with KIR2DL3 alleles that were nonreactive with anti-KIR2DL3 antibody clone 180701 (KIR2DL3\*005 or \*015 alleles). Logical gating was applied to estimate single KIR expressing NKc subsets (i.e. single-KIR2DS4: KIR2DS4<sup>+</sup> 2DL1<sup>-</sup> 2DS1<sup>-</sup> 2DL2S2<sup>-</sup> 2DL3<sup>-</sup> 3DL1<sup>-</sup> and 3DS1<sup>-</sup>, and so on).

**Figure 2. Functional KIR2SD4 is associated with IMV need and ICU admission.** A) Multivariate logistic regression analysis of IMV need and ICU admission of COVID-19 patients in relation to the

presence of KIR2DS4f and other variables significantly associated. B) Kaplan-Meier and Mantel-Haenszel log-rank tests for admission to ICU in relation to the presence of KIR2DS4f.

**Figure 3. Leukocyte subsets and expression of activating and inhibitory receptors on peripheral blood NKCs in COVID-19 patients and controls.** A) Percentage of total lymphocytes, monocytes and neutrophils (% with respect to total leukocyte), CD16<sup>+</sup> non-classical monocytes (% with respect to total monocytes) and CD4<sup>+</sup> and CD8<sup>+</sup> T cells and CD3-CD56<sup>+</sup> NKCs (% with respect to total lymphocytes) in healthy controls (white), COVID-19 patients that did (grey) or did not (black) require invasive mechanical ventilation (IMV). B) Percentage of KIR<sup>+</sup> NKc subsets (% with respect to total NKCs) in controls and patients. C) Mean fluorescence intensity (MFI) of inhibitory and activating KIR receptors on NKCs expressing each single KIR in controls and patients. D) MFI of inhibitory and activating KIR receptors on NKCs expressing each single KIR in presence (dotted bars) or absence (checked bars) of their respective HLA-ligand, C1, C2, Bw4, and HLA-A\*11/C\*02/C\*04/C\*05/C\*16 (KIR2DS4-ligands). E) MFI of CD226, CD16, CD56, TIGIT, NKG2A, and NKG2D on NKCs expressing single KIRs for controls and patients. ANOVA was used to compare controls with patients, or to compare expression of a particular receptor among different KIR<sup>+</sup> NKc subsets, \* p<0.05, \*\* p<0.01, \*\*\* p<0.001.

**Figure 4. KIR3DS1 is associated with HLA-B\*15:01 in COVID-19 patients.** A) KIR gene and KIR genotype frequencies in patients with HLA-B\*15 allotype and HLA-B\*15 subtypes. P estimated in Pearson's- $\chi^2$  and corrected (Pc) by the number of comparisons (x11). B) Computational prediction of KIR3DS1 (blue boxes) and KIR2DS1 (red box) interaction scores with different HLA-B\*15 allotypes presenting SARS-CoV-2 peptides. In each box plot, middle solid black lines indicate the median, edges the first and third quartiles, whiskers 1.5 interquartile range, and circles outliers of interaction score values. Black dashed line represents the score predicted for KIR3DL1/KIR3DS1 interaction with the Bw4 ligand. NetMHCpan-4.1 did not predict any strong binding SARS-CoV-2 peptide for HLA-B\*15:04 allotype. P-values: \* p<0.05, \*\* p<0.001, \*\*\* p<0.0001, NS p>0.05.

**Table 1. Patient characteristics distributed according to IMV need.**

	Total	No IMV	IMV	p
<b><u>Demographics</u></b>	<b>n=201</b>	<b>n=158 (78.6%)</b>	<b>n=43 (21.4%)</b>	
Age, years (mean±SD)	57.6±11.8	57.50±11.83	58.09±12.01	0.772
Female sex (%)	81 (40.3%)	69 (43.7%)	14 (32.6%)	0.255
Caucasian ethnicity (%)	166 (84%)	135 (88.2%)	29 (67.4%)	0.001
<b><u>Comorbidity and severity</u></b>				
Cardiovascular disease (%)	33 (16.1%)	19 (12.0%)	14 (32.6%)	0.003
Charlson score (mean±SD)	1.41±1.84	1.28±1.84	1.88±1.79	0.059
SOFA (mean±SD)	2.41±3.03	1.34±2.01	6.87±2.44	0.001
SOFA > 6 (%)	35 (17.9%)	8 (5.1%)	27 (71.1%)	0.001
CURB65 (mean±SD)	1.02±1.21	0.64±0.89	2.58±1.08	0.001
CURB65 > 2 (%)	55 (28.2%)	22 (14.0%)	33 (86.8%)	0.001
PaO <sub>2</sub> /FiO <sub>2</sub> (mean±SD)	131.04±78.79	148.5±86.46	107.3±60.29	0.012
SaO <sub>2</sub> /FiO <sub>2</sub> (mean±SD)	379.9±104.4	304.6±151.8	140.3±90.12	0.001
<b><u>Blood analysis</u></b>				
Calcium mg/dl (mean±SD)	9.26±0.59	9.34±0.49	8.95±0.81	0.001
ALT U/L (mean±SD)	51.25±309.77	29.42±24.73	134.32±677.42	0.053
LDH U/L (mean±SD)	384.47±864.25	323.3±150.5	619.9±1880.4	0.053

Ferritin ng/ml (mean±SD)	261.34±483.8	191.6±394.8	523.2±670.7	0.001
Albumin mg/dl (mean±SD)	4.23±0.67	4.39±0.43	3.62±1.01	0.001
Hemoglobin g/dl(mean±SD)	13.05±2.10	13.52±1.75	11.25±2.34	0.001
Lymphocytes (mean±SD)	1870.1 ±685.1	1922.1±592.9	1667.7±947.0	0.036
CRP ng/ml (mean±SD)	1.34±4.01	0.53±0.92	4.33±7.88	0.001
D. Dimer ng/ml (mean±SD)	589.03±719.3	508.6±617.1	885.2±963.2	0.003
<b><u>Treatments</u></b>				
Remdesivir (%)	15 (7.5%)	7 (4.4%)	8 (18.6%)	0.005
Tocilizumab (%)	44 (21.9%)	22 (13.9%)	22 (52.4%)	0.001
Steroids (%)	71 (35.3%)	43 (27.2%)	28 (65.1%)	0.001
<b><u>Clinical evolution</u></b>				
Acute kidney failure (%)	24 (13%)	4 (2.7%)	20 (54.1%)	0.001
ARDS (%)	100 (49.8)	57 (36.1%)	43 (100.0%)	0.001
Admission to ICU (%)	85 (42.3)	42 (26.6%)	43 (100.0%)	0.001
Days to hospital (mean±SD)	8.14±5.2	8.60±5.38	7.00±4.57	0.088
Days to ICU (mean±SD)	8.78±4.5	9.53±3.91	7.95±4.99	0.111
Days of stay (mean±SD)	21.3±10.84	15.10±13.59	37.76±22.2	0.001
Abbreviations: IMV: Invasive Mechanical Ventilation; SOFA: Sepsis-related Organ Failure Assessment, CURB-65: Severity Score for Community-Acquired Pneumonia; ARDS: Acute Respiratory Distress Syndrome; ICU: Intensive Care Unit; ALT: alanine transaminase; LDH: lactate dehydrogenase, SD: standard deviation.				

- No significant differences were found for: body mass index (30.3 vs. 28.5 index), smoking (23.3% vs. 19%), hypertension (51.2% vs. 35.4%), diabetes mellitus (20% vs. 15.8%), cerebrovascular disease (4.7% vs. 4.4%), chronic bronchitis (9.3% vs. 5.0%), asthma (2.3% vs. 11.4%), chronic kidney failure (4.8% vs. 6.3%), cancer (9.3% vs. 9.5%), treatments with lopinavir-ritonavir (37.4% vs. 40.5%), hydroxichloroquine (65.1% vs. 54.4%), or azithromycin (62.8% vs. 58.9%); glucose levels (113.6 vs. 108.9 mg/dl), creatinine (0.82 vs. 0.88 mg/dl), phosphorus (4.12 vs. 3.83 mg/ml), bilirubin (1.31 vs. 1.69 mg/ml), creatine phosphokinase (85.1 vs. 80.1 U/L)

- Control group (n=210): Caucasian (89.0%), sex (male 45%), and age (53.0±12.1).

Accepted Manuscript

**Table 2. KIR and KIR-ligand (HLA-I) frequencies in the study groups**

	<b>Controls</b>	<b>Covid-19</b>	<b>Cv19 noIMV</b>	<b>Cv19 IMV</b>
<b>KIR genes</b>	(n=210)	(n=201)	(n=158)	(n=43)
KIR2DL1	200 (95.2%)	194 (96.5%)	153 (96.8%)	41 (95.3%)
KIR2DL2	117 (55.7%)	102 (50.7%)	78 (49.4%)	24 (55.8%)
KIR2DL3	187 (89.0%)	181 (90.0%)	143 (90.5%)	38 (88.4%)
KIR2DL5	116 (55.2%)	114 (56.7%)	89 (56.3%)	25 (58.1%)
KIR3DL1	193 (91.9%)	184 (91.5%)	142 (89.9%)	42 (97.7%)
KIR2DS1	94 (44.8%)	87 (43.3%)	70 (44.3%)	17 (39.5%)
KIR2DS2	119 (56.7%)	101 (50.2%)	78 (49.4%)	23 (53.5%)
KIR2DS3	62 (29.5%)	60 (29.9%)	49 (31.0%)	11 (25.6%)
KIR2DS4	193 (91.9%)	183 (91.0%)	141 (89.2%)	42 (97.7%)
dKIR2DS4	166 (79.0%)	155 (77.1%)	124 (78.5%)	31 (72.1%)
fKIR2DS4	76 (36.2%)	124 (61.7%) <sup>a</sup>	88 (55.7%)	36 (83.7%) <sup>b</sup>
KIR2DS5	180 (29.3%)	68 (33.8%)	55 (34.8%)	13 (30.2%)
KIR3DS1	253 (41.1%)	86 (42.8%)	69 (43.7%)	17 (39.5%)
<b>Centromeric-genotype</b>				
AA	93 (44.3%)	99 (49.3%)	80 (50.6%)	78 (49.4%)

Bx	117 (55.7%)	102 (50.7%)	78 (49.4%)	21 (60.0%)
<b>Telomeric-genotype</b>				
AA	118 (56.2%)	115 (57.2%)	89 (56.3%)	26 (60.5%)
Bx	92 (43.8%)	86 (42.8%)	69 (43.7%)	17 (39.5%)
<b>HLA-I KIR-ligand</b>				
C1	117 (85.5%)	168 (83.6%)	130 (82.3%)	38 (88.4%)
C2	135 (65.2%)	139 (69.2%)	113 (71.5%)	26 (60.5%)
Bw4	149 (75.3%)	145 (72.1%)	115 (72.8%)	30 (69.8%)
KIR2DS4-ligands <sup>c</sup>	129 (62.3%)	131 (65.2%)	105 (66.5%)	26 (60.5%)

Abbreviations: KIR: Killer-cell Immunoglobulin-like receptor; fKIR2DS4: functional-KIR2DS4; KIR2DS4: deleted-exon5-KIR2DS4; HLA: Human Leukocyte Antigen. <sup>a</sup> Control vs. Covid-19,  $P < 6.8 \times 10^{-7}$  ( $P_c < 9.5 \times 10^{-6}$ ); <sup>b</sup> IMV vs. no-IMV,  $P < 0.001$ ; <sup>c</sup> KIR2DS4-ligands: HLA-A\*11, C\*2, C\*4, C\*5, and C\*16 [35]. P values estimated with Chi-Square.  $P_c$  = p-value after Bonferroni correction (x14).

**Table 3. Clinical characteristics and evolution of patients in relation to fKIR2DS4.**

	No fKIR2DS4 n=77 (38.3%)	fKIR2DS4 n=124 (61.7%)	p
<b>Demographics</b>			
Age (Mean±SD, Years)	57.7±10.8	57.8±12.5	0.947
Sex (Female %)	36.4%	41.9%	0.263
Ethnicity (Caucasian %)	87.0%	83.9%	0.347
<b>Clinical characteristics</b>			
Asthma (%)	12 (15.6%)	7 (5.6%)	0.036
SOFA (mean±SD)	1.67±2.17	2.88±3.40	0.006
SOFA > 6 (%)	6 (7.9%)	29 (24.2%)	0.007
CURB65 (mean±SD)	0.84± 1.09	1.12±1.27	0.109
PaO <sub>2</sub> /FiO <sub>2</sub> (mean±SD)	142.5±76.7%	124.9±79.8	0.309
<b>Evolution</b>			
Days to hospital admission (mean±SD)	9.40±5.79	7.36±4.66	0.019

Days to admission to ICU (%)	25 (32.5%)	60 (48.4%)	0.038
Acute kidney failure (%)	4 (5.6%)	20 (17.7%)	0.030
Days of stay (mean±SD)	16.6±14.04	23.7±21.15	0.031

---

Abbreviations: fKIR2DS4: functional-KIR2DS4; SOFA: Sepsis-related Organ Failure Assessment, CURB-65: Severity Score for Community-Acquired Pneumonia; ARDS: Acute Respiratory Distress Syndrome; ICU: Intensive Care Unit. No differences were observed for the rest of variables described in table 1.

Accepted Manuscript

Figure 1

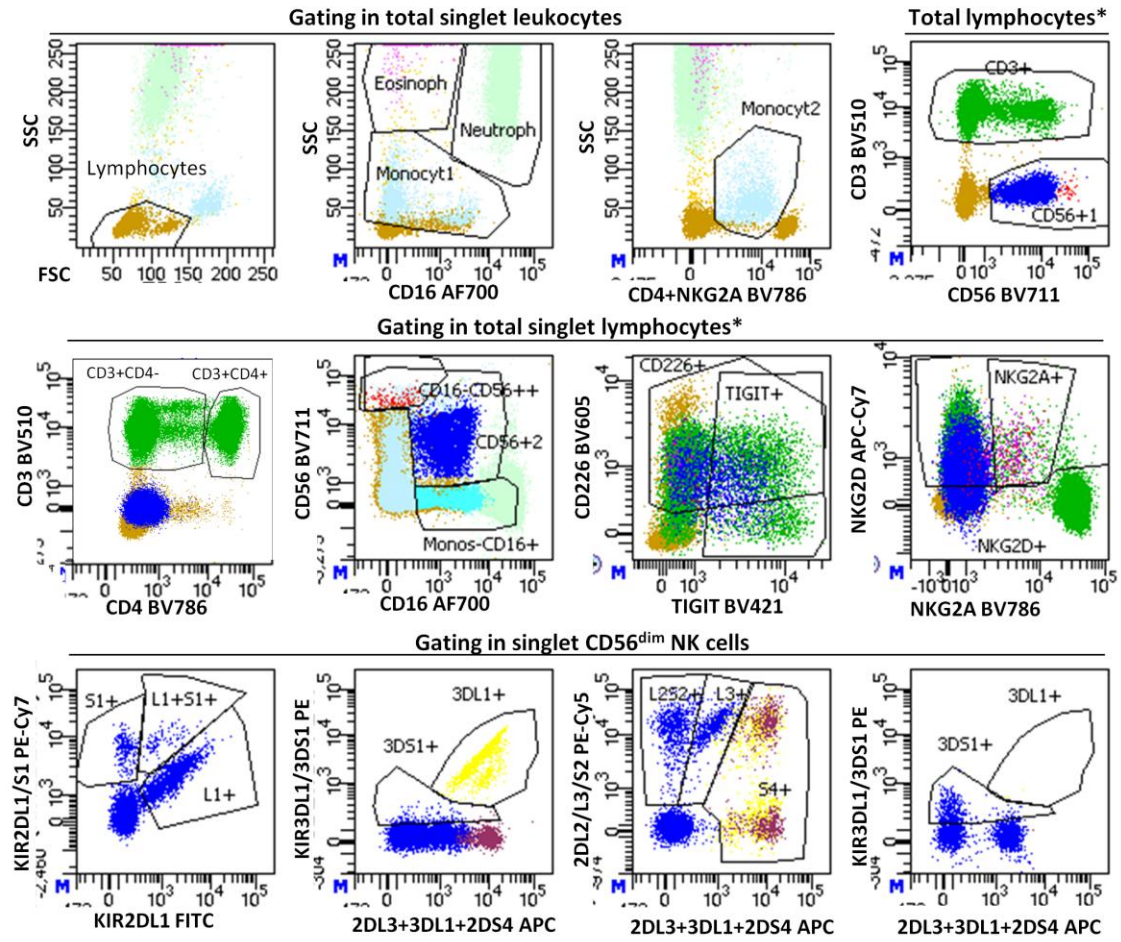


**Figure 2**

**A Multivariate logistic regression analysis for variables associated to IMV requirement<sup>1</sup>**

Variable	OR	95% CI	p
Functional KIR2DS4	4.74	1.76-12.79	0.002
Cardiovascular D.	4.23	1.65-10.85	0.003
Ferritin	1.001	1-1.002	0.005
D-Dimer	1.001	1-1.002	0.008

**Multivariate logistic regression analysis associated to ICU admission<sup>1</sup>**

Variable	OR	95% CI	p
Functional KIR2DS4	2.51	1.087-5.82	0.031
Cardiovascular D.	3.94	1.31-11.86	0.014
D-Dimer	1.001	1-1.002	0.005

<sup>1</sup> Age, sex, arterial hypertension, and obesity were also included, without significant results.

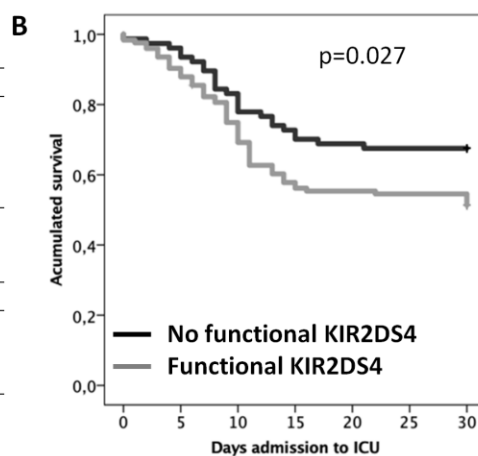


**Figure 3**

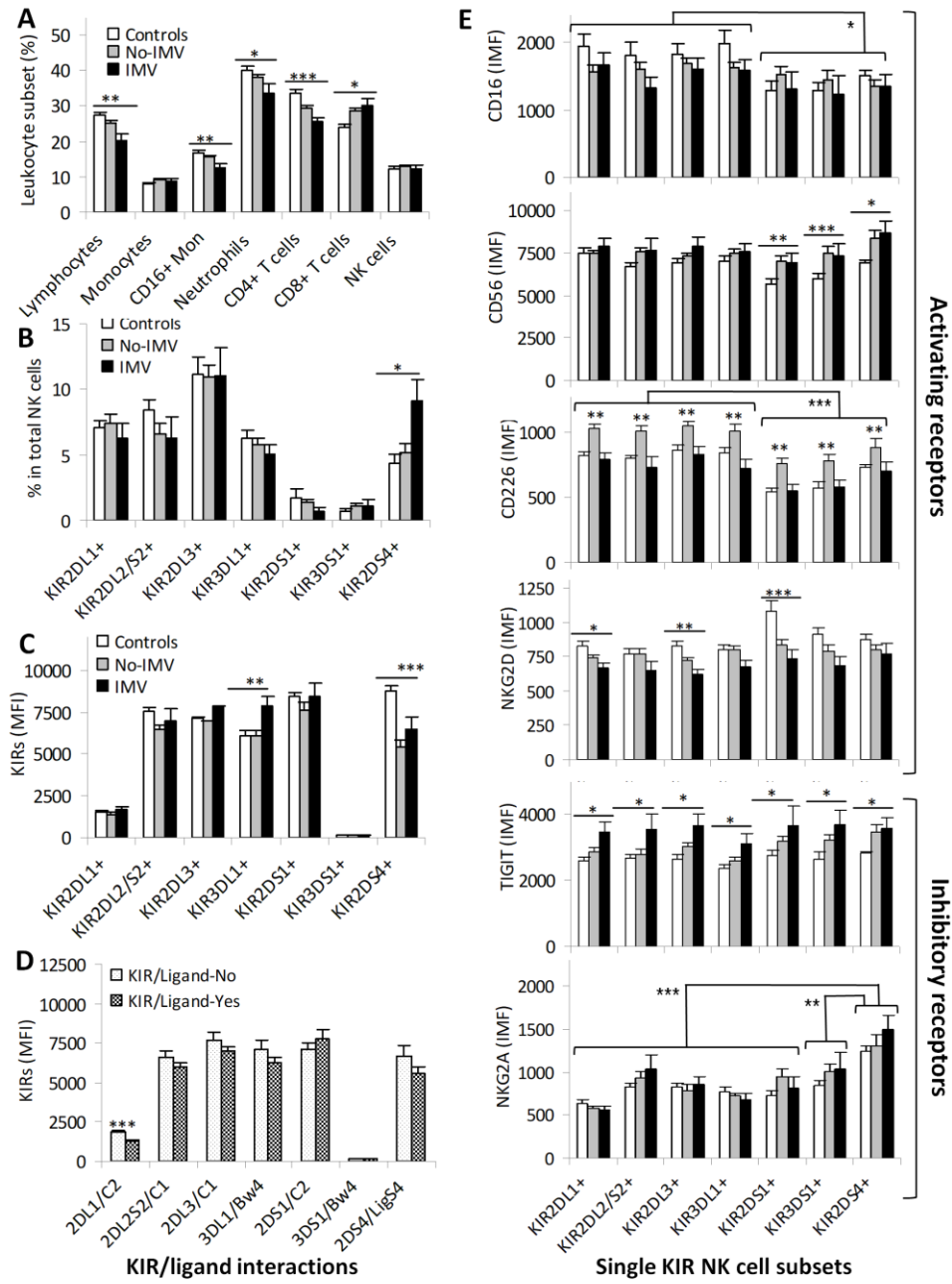


Figure 4

